



## Nano Metal-Organic Framework Particles (*i.e.* MIL-100(Fe), HKUST-1(Cu), Cu-TPA, and MOF-5(Zn)) using a Solvothermal Process

Asep Bayu Dani Nandiyanto

Departemen Kimia, Universitas Pendidikan Indonesia, Jl. Dr. Setiabudi no 229, Bandung 40154, Indonesia

Correspondence: E-mail: [nandiyanto@upi.edu](mailto:nandiyanto@upi.edu)

### ABSTRACT

Metal-organic framework (MOF) is attractive because of its representation as a class of crystalline porous materials with excellent properties, specifically its chemical functionality and high porosity, making it potentially tailored for various desired applications. Although the synthesis of MOFs have been well-documented, most reports are in the bulk and micrometer sizes. The synthesis of MOFs in the smaller size is still inevitable. This work reports the synthesis of nano MOF particles (*i.e.*, MIL-100(Fe), HKUST-1(Cu), Cu-TPA, and MOF - 5 (Zn)). In the experiment, MOFs were created by interacting ligands and metal ions in the specific solvent in the solvothermal process. Different from other reports, this study used low concentrations of ligands and metal ions, in which this is effective to control ligand-metal ion interaction, reaction, nucleation, and growth of MOF. The successful synthesis was obtained and effective for various MOF particles by changing types of ligands and metal ions. The study also obtained that compatibility and dilution of the ligands and the metal ions in the specific solvent are important parameters. This information will bring new strategies and further developments for the synthesis of MOF materials for wider range of potential applications in separation, catalysis, dye adsorption, and drug carrier uses.

### ARTICLE INFO

**Article History:**

*Submitted/Received 01 Feb 2019*

*First revised 11 Apr 2019*

*Accepted 11 Jun 2019*

*First available online 15 Jun 2019*

*Publication date 01 Sep 2019*

**Keywords:**

*Metal organic framework,*

*Particle synthesis,*

*Ligand,*

*Metal ion,*

*Powder technology,*

*Chemical education.*

## 1. INTRODUCTION

Metal-organic framework (MOF) materials have emerged as an excellent material with ultrahigh porosity (up to 90% free volume) and enormous internal surface areas. The surface area can extend beyond 6000 m<sup>2</sup>/g. When these properties combined together with other various properties, it makes MOF materials to be applicable for prospective applications in clean energy, most significantly as separation and storage media for gases such as hydrogen and methane. In addition, MOF is also possibly applied for membranes, thin-film devices, catalysis, and biomedical imaging (Zhou *et al.*, 2012).

The numbers of review articles and monographs have been documented for the escalation of the MOF material synthesis. In short, MOF material was produced by interacting ligands and metal ions in a specific solvent (Lee *et al.*, 2009). MOFs have been available mostly in micron and millimeter size, and reports on the production of MOFs in smaller sizes are still inevitable.

Here, the purpose of this study was to simply comprehend and investigate the facile synthesis of nano-sized MOF particles. To assist the production of MOF materials, solvothermal process was used. Various types of ligands and metal ions were tested to form various types of MOF particles (see **Table 1**). The present study also investigated the interaction of ligands and metal ions systematically. Then, the results were tested and examined by several characterizations, *i.e.*, a scanning electron microscope (SEM) and an X-ray diffraction (XRD).

In addition, to evaluate the effect of combination of ligands and metal ions on the formation of MOF material, various ligands and metal ions were tested, which were used

to form various types of MOF materials, *i.e.*, MIL-100(Fe), HKUST-1(Cu), Cu-TPA, and MOF-5(Zn). These types of MOF materials were selected as the models of MOF materials since they have been classified as one of the most popular MOF materials. Indeed, this will bring other prospective innovations in the further development of MOF materials with their wider range of potential applications in separation, catalysis, dye adsorption, and drug carrier uses.

## 2. MATERIALS AND METHODS

### 2.1. Chemicals

Iron (III) chloride (FeCl<sub>3</sub>·6H<sub>2</sub>O), iron (III) nitrate (Fe(NO<sub>3</sub>)<sub>3</sub>·6H<sub>2</sub>O), Iron (II) chloride (FeCl<sub>2</sub>·6H<sub>2</sub>O), copper (II) nitrate (Cu(NO<sub>3</sub>)<sub>2</sub>·6H<sub>2</sub>O), and zinc nitrate (Zn(NO<sub>3</sub>)<sub>2</sub>·6H<sub>2</sub>O) were used as metal sources. Trimesic acid (TMA) and Terephthalic acid (TPA) were used as ligand components. These chemicals were used for the preparation of various types of MOF materials, *i.e.*, MIL-100(Fe), HKUST-1(Cu), Cu-TPA, and MOF-5(Zn). Dimethyl formamide (DMF) was also used as a solvent dissolution agent for removing unreacted chemicals. All chemicals were purchased from Sigma-Aldrich US and used without further purification.

### 2.2. Synthesis procedure

For the synthesis of MOF materials, ligands were initially diluted in the solvent (concentration of 120 mmol/L). Subsequently, metal sources was inserted into the solution, mixed, and kept in room temperature for about 15 minutes. Next, the mixed solution was introduced into the solvothermal process using the conventional solvothermal apparatus. In short, the apparatus consisted of 150 mL of PTFE reactor with inner reactor with dimensions for diameter and height of 35 and 90 mm, respectively. The teflon reactor was

equipped with solvothermal metal blanket (stainless steel reactor).

For starting the synthesis process, the apparatus contained ligands and metal ions was introduced to the furnace at a temperature of 150°C for 12 hours. Please see detailed information regarding the experimental setup in **Figure 1**. In this study, the mole ratio of ligands and metal ions was fixed at 1.00. The list of chemicals used for

the formation of MOF materials is shown in **Table 1**.

After the reaction process, the product was purified using a centrifugation process (three times at 11,000 rpm for 30 minutes and washed with DMF). This centrifugation process was used for removing unreacted chemicals. The centrifuged product was then dried in a vacuum oven at temperature of 50°C overnight for characterization and use.

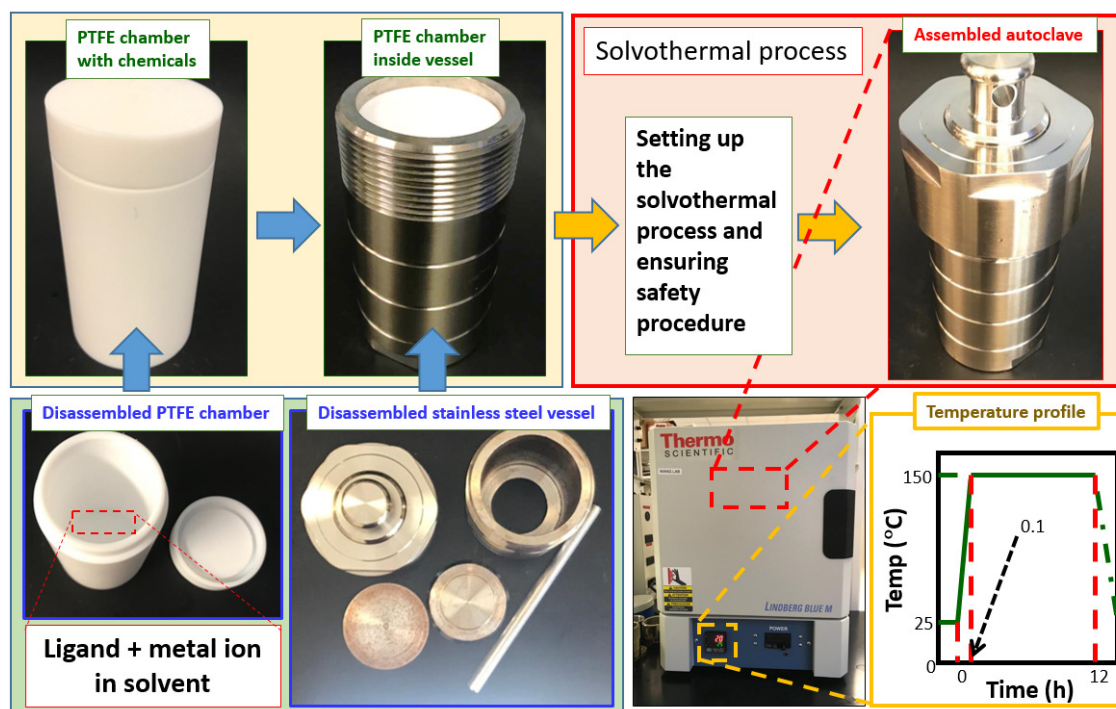


**Figure 1.** Experimental setup.

**Table 1.** Mean abrasion weight losses of high-performance DSP cementitious mortars with nano- and/or micro-scale reinforcement.

Sample	Ligand	Metal ion raw material	Solvent	Product
A	TMA	FeCl <sub>3</sub> .6H <sub>2</sub> O	UPW	MIL-100(Fe)
B	TMA	FeCl <sub>2</sub> .6H <sub>2</sub> O	UPW	MIL-100(Fe)
C	TMA	Fe(NO <sub>3</sub> ) <sub>3</sub> .6H <sub>2</sub> O	UPW	MIL-100(Fe)
D	TMA	Cu(NO <sub>3</sub> ) <sub>2</sub> .6H <sub>2</sub> O	UPW	HKUST-1(Cu)
E	TMA	CuCl <sub>2</sub> .6H <sub>2</sub> O	UPW	HKUST-1(Cu)
F	TPA	FeCl <sub>3</sub> .6H <sub>2</sub> O	UPW	Iron oxide
G	TPA	Cu(NO <sub>3</sub> ) <sub>2</sub> .6H <sub>2</sub> O	UPW	Unsuccessful
H	TPA	Zn(NO <sub>3</sub> ) <sub>2</sub> .6H <sub>2</sub> O	UPW	Unsuccessful
I	TPA	FeCl <sub>3</sub> .6H <sub>2</sub> O	Methanol	Iron oxide
J	TPA	Cu(NO <sub>3</sub> ) <sub>2</sub> .6H <sub>2</sub> O	Methanol	Cu-TPA
K	TPA	Zn(NO <sub>3</sub> ) <sub>2</sub> .6H <sub>2</sub> O	Methanol	MOF-5

### 2.3. Characterizations

Several characterizations were conducted: (i) SEM (Hitachi SU-70, Hitachi Co Ltd., Japan) equipped with EDX measurement for analyzing the morphology and size of particles; and (ii) X-ray diffraction (XRD, PANalytical X'Pert Pro MPD X-ray diffractometer using Cu-K $\alpha$  radiation) for analyzing the crystal structure.

## 3. RESULTS AND DISCUSSION

### 3.1. Turpis egestas

**Figure 2** depicts the analysis of the synthesis of MOF particles prepared using TMA (as a ligand) with various Fe sources (as a metal ions) using the solvothermal method. **Figures 2(a), (b), and (c)** are the SEM images samples prepared from combination of TMA and various Fe sources (*i.e.*, FeCl<sub>3</sub>, Fe(NO<sub>3</sub>)<sub>3</sub>, and FeCl<sub>2</sub>, respectively; detailed combination is shown as **samples A, B, and C** in **Table 1**). The SEM images confirmed that samples contained particles with sizes from nano to submicron, demonstrating that the combination of TMA and various types of Fe ions in this low concentration (*i.e.*, 120 mmol/L) is effective to create nanoparticles. The ferret analysis showed that the particles prepared with FeCl<sub>3</sub>, Fe(NO<sub>3</sub>)<sub>3</sub>, and FeCl<sub>2</sub> have sizes of about 200, 400, and 100 nm, respectively.

XRD analysis in **Figure 2(d)** showed that the present combination of TMA and various Fe sources have identical XRD patterns for MIL-100(Fe) materials, confirmed by the simulated XRD pattern of MIL-100(Fe) and current literature ([Hei et al., 2014](#)).

The study also found the followed phenomena. Since FeCl<sub>3</sub> and Fe(NO<sub>3</sub>)<sub>3</sub> can

create Fe<sup>3+</sup> ions, it should be no effect of the interaction and reaction between Fe ions and TMA on the formation of MIL-100(Fe). However, different final particle sizes were found (see different particle morphologies in **Figures 2(a) and (b)**). The main reason for the different sizes are due to the impact of anions on the substitution of H<sup>+</sup> in TMA molecules by Fe ions and oxygen elements. Cl<sup>-</sup> ions disturb more than NO<sub>3</sub><sup>-</sup> ions. In fact, substitution of Fe ions into the deprotonation of TMA have a direct impact to the nucleation and growth rate of the MOF materials. The use of FeCl<sub>3</sub> has higher nucleation rate (more nuclei to be formed) than that of Fe(NO<sub>3</sub>)<sub>3</sub>. The reactant would rather create more new nuclei than grow to increase the weight of the formed nuclei.

In the case of FeCl<sub>2</sub> that can form Fe<sup>2+</sup> ions, smaller particles were obtained compared to the process using FeCl<sub>3</sub>. The types of anions (*i.e.*, Cl<sup>-</sup>) in both chemicals were the same, and the type of XRD pattern are identical. The main fundamental reason for the different sizes is due to the type of Fe ion in converting H<sup>+</sup> in the TMA. Fe<sup>2+</sup> has more active to attack and collaborate with TMA to form MIL-100(Fe) than Fe<sup>3+</sup>. Further, atomic scale for the Fe<sup>2+</sup> is smaller than Fe<sup>3+</sup>. As a result, the increases in the nucleation rate could be obtained. However, the size distribution of the sample prepared with Fe<sup>2+</sup> is broader than that with Fe<sup>3+</sup>. This is because of the need for reconstruction of the crystal system to obtain the most stable structure. The circumstance in the missing one positive ion in the Fe ion (from Fe<sup>3+</sup> to Fe<sup>2+</sup>) has an impact to the MOF crystal to form the most stable crystal structure.

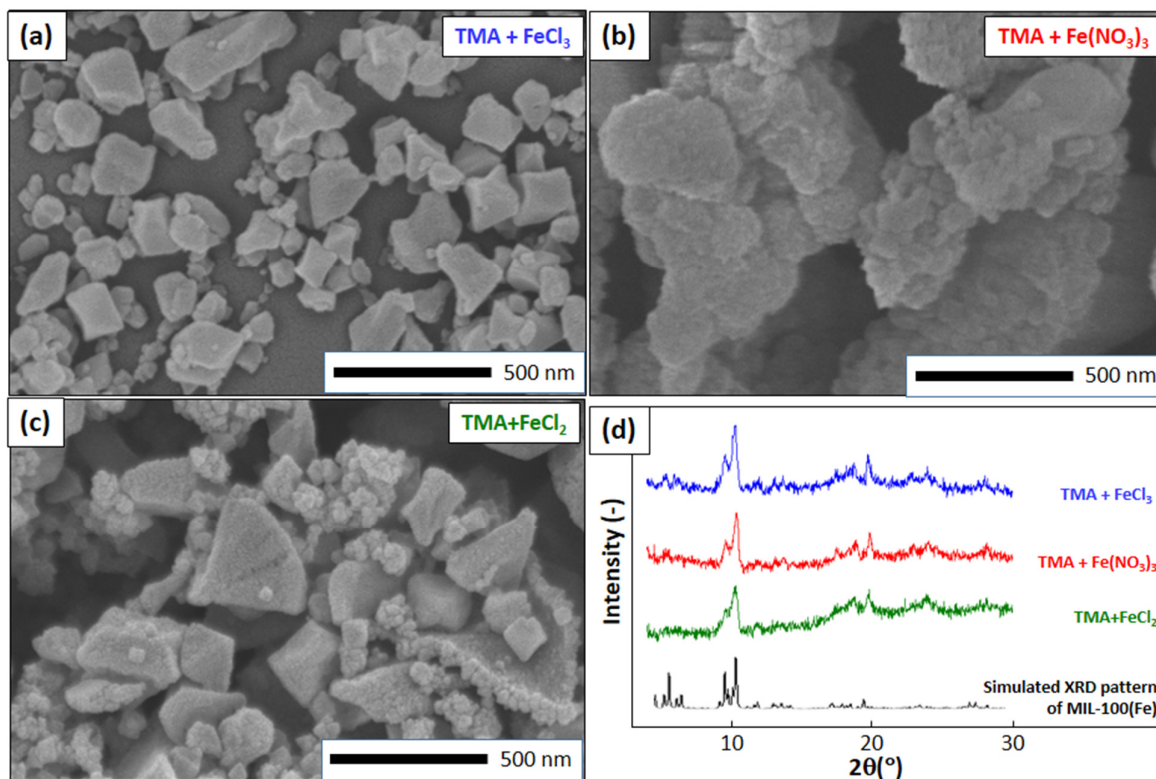


**Figure 2.** Analysis results of samples prepared with various types of Fe ions using the solvothermal method. Figures (a), (b), and (c) are the SEM images of samples prepared with TMA and  $\text{FeCl}_3$ ,  $\text{Fe}(\text{NO}_3)_3$ , and  $\text{FeCl}_2$ , respectively. Figure (d) is the XRD analysis results. Figure (a) was adopted from reference (Nandiyanto *et al.*, 2019).

To confirm the effect of anionic on the control of particle size, **Figure 3** shows the analysis results of samples prepared with TMA and various types of Cu ions using the solvothermal process (see **samples D and E** in **Table 1**). Two types of Cu sources were used:  $\text{CuCl}_2$  and  $\text{Cu}(\text{NO}_3)_2$ . The SEM images presented that the  $\text{CuCl}_2$  led to the formation of larger particles compared to  $\text{Cu}(\text{NO}_3)_2$  (see **Figures 3(a) and (b)**, respectively). The XRD analysis results in **Figure 3(c)** confirmed that the changes in the types of Cu ions have no impact on the change in crystalline structure of the HKUST-1 material, and the XRD patterns are identical to the samples that prepared using a conventional method (Venkatasubramanian *et al.*, 2010).

The analysis results for the sizes based on SEM results in **Figures 3(a) and (b)** are not in a good agreement with the above data in **Figure 2**. The main reason for the opposite trends is because the size of Cu (0.120 nm for covalent type Cu) is larger than that of Fe (0.102 nm for covalent type Cu). In the formation of MOFs, The  $\text{Cl}^-$  ions seem to be unable to give impact on shifting the Cu ions, while  $\text{NO}_3^-$  ion is large enough to make shifting the Cu ions. As a result,  $\text{NO}_3^-$  becomes the most disturbing component that brings great impacts on disturbing substitution of  $\text{H}^+$  by Cu ions.



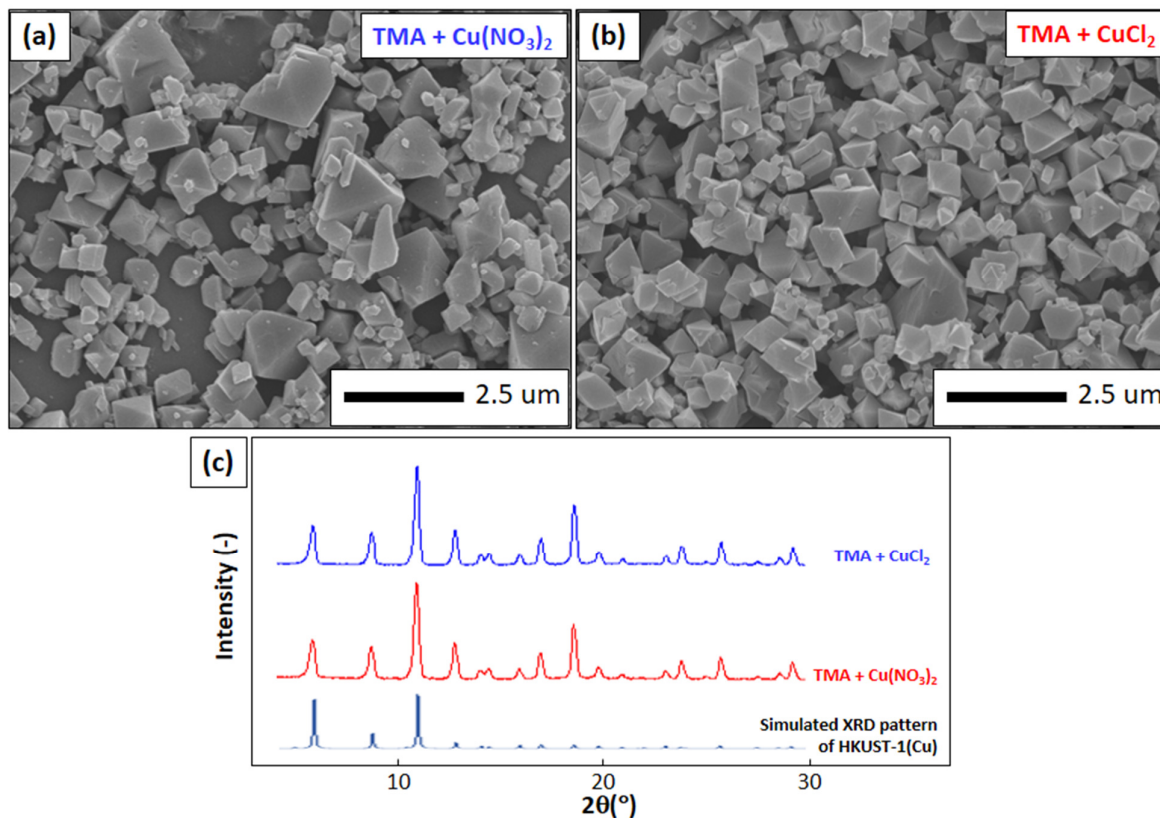


**Figure 3.** The SEM (a,b) and XRD (c) analysis results of samples prepared with TMA and various Cu ions using the solvothermal synthesis method. Figures (a) and (b) are samples prepared using  $\text{CuCl}_2$  and  $\text{Cu}(\text{NO}_3)_2$ , respectively.

To confirm the effectiveness of the present method on the formation of other types of MOF materials, we also used TPA as the ligand component. We found that the preparation of samples prepared with TPA and various metal ions in aqueous solution (see **samples F, G, and H** in **Table 1**) did not create MOF materials. The main reason is due to the low dissolution of TPA in the aqueous solution.

To address the above problem, **Figure 4** presents the analysis results of the samples prepared with TPA and various types of ions (see **samples I, J, and K** in **Table 1**) in methanol solution. The SEM images in **Figures 4(a)-(d)** showed particles with sizes of from nanometer. The XRD analysis results in **Figure 4(e)** showed that the use of TPA in methanol solution is not completely good for preparing MOF materials. Although some

MOFs can be created when conducting process in **samples G and H**, the product still containing impurities and byproduct. Further, the process using a precursor containing  $\text{FeCl}_3$  seemed to be failure in creating MOF materials. Instead of the formation MOF materials, the sample create amorphous materials with iron oxide component (*Chiou et al., 2013*). The sample that used  $\text{Cu}(\text{NO}_3)_2$  has some  $\text{Cu}(\text{OH})_2$  (*Wang et al., 2014*), whereas sample with  $\text{Zn}(\text{NO}_3)_2$  has ZnO (*Zhang et al., 2002*) and zinc terephthalate dehydrate (*Rodríguez et al., 2015*). In addition, the combination of TPA and  $\text{Zn}(\text{NO}_3)_2$  also creates specific MOF-water composite (*Rodríguez et al., 2015*), as assigned at wavenumbers of about 9 and 18°. These results strengthened the hypothesis that to form nano MOFs, ligands and metal ions must be well-dissolved. Otherwise, the

ligand-metal ion interaction cannot be done. Thus, it is required to find out an appropriate solvent.

In addition, in the case of TPA, TPA is well-dissolved into the DMF. However, the DMF is classified as a hazardous chemical (Yang *et al.*, 2014). Further, adding DMF into the solvothermal process relates to the additional heat and pressure, resulting shortcomings in the handling process.

Based on the above results, the main ideas gained from this study is to get successful synthesis of smaller-sized MOF materials (Bosch *et al.*, 2014). several factor

must be considered. The factors are (1) the use of low-concentration ligands and metal ions to enhance nucleation rate; (2) the condition for making well dispersion of ligands and metal ions in the solvent. Thus, finding a good solvent that can dissolve these reactants is important; (3) optimization of concentrations of ligands and metal ions in the solution. Optimization will lead to the typical reaction happening during the process as well as the formation of the material (Marimpul, 2017; Muslih *et al.*, 2017; Nordin *et al.*, 2018); and (4) the compatibility between ligands and metal ions to form MOFs.

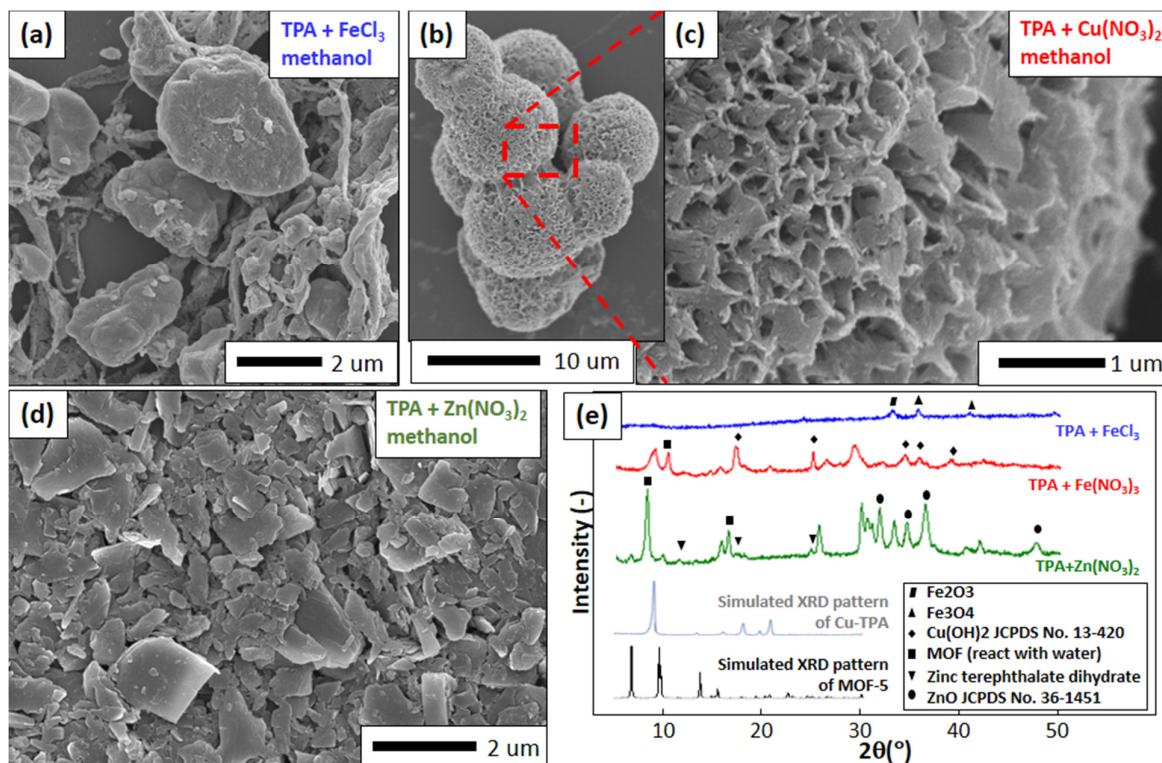


**Figure 4.** The SEM (a-d) and XRD (e) analysis results of samples prepared with TPA and various types of metal ions using the solvothermal synthesis method. Figures (a), (b-c), and (d) are samples prepared using  $\text{FeCl}_3$ ,  $\text{Cu}(\text{NO}_3)_2$ , and  $\text{Zn}(\text{NO}_3)_2$ , respectively. Figures (b) and (c) are the low- and high-magnified SEM images of samples prepared using  $\text{Cu}(\text{NO}_3)_2$ .

#### 4. CONCLUSION

The present study has successfully demonstrated for the formation of nano-sized MOF particles (*i.e.*, MIL-100(Fe), HKUST-1(Cu), Cu-TPA, and MOF-5(Zn)) using the solvothermal processing method. Various types of ligands and metal ions, as well as solvents were tested. The experimental results showed that to get successful synthesis of smaller-sized MOF particles, several factors must be considered: (1) the use of low-concentration ligands and metal ions to enhance nucleation rate; (2) the condition for making well dispersion of ligands and metal ions in the solvent; (3) optimization of concentrations of ligands and metal ions in the solution; and (4) the

compatibility between ligands and metal ions to form MOFs.

#### 5. ACKNOWLEDGEMENTS

A.B.D.N. acknowledged RISTEK DIKTI Fulbright fellowship. We thank to Dr. Wei-Ning Wang for supporting this research. A.B.D.N. also acknowledged PTUPT, PSNI, and WCR research grant from RISTEK DIKTI.

#### 6. AUTHORS' NOTE

The author(s) declare(s) that there is no conflict of interest regarding the publication of this article. Authors confirmed that the data and the paper are free of plagiarism.

#### 7. REFERENCES

- Bosch, M., Zhang, M., and Zhou, H.-C. (2014). Increasing the stability of metal-organic frameworks. *Advances in Chemistry*, 2014, 1-8.
- Chiou, J.-R., Lai, B.-H., Hsu, K.-C., and Chen, D.-H. (2013). One-pot green synthesis of silver/iron oxide composite nanoparticles for 4-nitrophenol reduction. *Journal of Hazardous Materials*, 248, 394-400.
- Hei, S., Jin, Y., and Zhang, F. (2014). Fabrication of  $\gamma$ -Fe<sub>2</sub>O<sub>3</sub> nanoparticles by solid-state thermolysis of a metal-organic framework, MIL-100 (Fe), for heavy metal ions removal. *Journal of Chemistry*, 2014, 1-6.
- Marimpul, R. (2017). Effect of substrate temperature on quality of copper film catalyst substrate: A Molecular Dynamics Study. *Indonesian Journal of Science and Technology*, 2(2), 183-190.
- Muslih, E. Y., Ismail, A., and Kim, K. H. (2017). Synthesis CuInSe<sub>2</sub> (CISe) Thin Films Prepared from Metal-Ethanolamine Complex Compound. *Indonesian Journal of Science and Technology*, 2(2), 191-196.
- Nandiyanto, A. B. D., He, X., and Wang, W.-N. (2019). Colloid-Assisted Growth of Metal-Organic Framework Nanoparticles. *CrystEngComm*, 21(14), 2268-2272.
- Nordin, N. A. H. M., Ismail, A. F., Racha, S. M., Cheer, N. B., Bilad, M. R., Putra, Z. A., and Wirzal, M. D. H. (2018). Limitation in Fabricating PSf/ZIF-8 Hollow Fiber Membrane for CO<sub>2</sub>/CH<sub>4</sub> Separation. *Indonesian Journal of Science and Technology*, 3(2), 138-149.
- Rodríguez, N. A., Parra, R., and Grela, M. A. (2015). Structural characterization, optical properties and photocatalytic activity of MOF-5 and its hydrolysis products: implications on their excitation mechanism. *RSC Advances*, 5(89), 73112-73118.
- Lee, J., Farha, O. K., Roberts, J., Scheidt, K. A., Nguyen, S. T., and Hupp, J. T. (2009). Metal-organic framework materials as catalysts. *Chemical Society Reviews*, 38(5), 1450-1459.



- Yang, N., Chen, X., Lin, F., Ding, Y., Zhao, J., and Chen, S. (2014). Toxicity formation and distribution in activated sludge during treatment of N, N-dimethylformamide (DMF) wastewater. *Journal of Hazardous Materials*, 264, 278-285.
- Venkatasubramanian, A., Lee, J.-H., Houk, R. J., Allendorf, M. D., Nair, S., and Hesketh, P. J. (2010). Characterization of HKUST-1 crystals and their application to MEMS microcantilever array sensors. *ECS Transactions*, 33(8), 229-238.
- Wang, L., Zhang, K., Hu, Z., Duan, W., Cheng, F., and Chen, J. (2014). Porous CuO nanowires as the anode of rechargeable Na-ion batteries. *Nano Research*, 7(2), 199-208.
- Zhang, J., Sun, L., Liao, C., and Yan, C. (2002). A simple route towards tubular ZnO. *Chemical Communications*(3), 262-263.
- Zhou, H.-C., Long, J. R., and Yaghi, O. M. (2012). Introduction to metal–organic frameworks. *Chemical Reviews*, 112(2), 673-674.